〈논 문〉 SAE NO. 97370069

A Mathematical Model of a Power Steering System

파워 스티어링 시스템의 수학적 모델에 관한 연구

장 봉 춘*, 이 성 철**
B. C. Jang, S. C. Lee

ABSTRACT

The focus of this research is to set up and describe the mathematical derivation of an automobile power-assisted rack and pinion steering system dynamics. The mathematical model of the power steering system dynamics with a 5 DOF linear vehicle model will be used in the computer simulation and evaluated comparing with the experimental results. This model is flexible to accommodate different vehicles through simple parameter changes. The developed mathematical model will attempt to provide enhanced driver realism to a Systems Technology, Inc. driving SIMulator(STISIM).

주요기술용어 : Rack and pinion type power steering(랙-피니언 형 파워스티어링), Linear vehicle model(선형 차량 모델), Driver realism(운전자 사실주의), STI driving simulator (STI사 모의 조향장치)

NOMENCLATURE

Dynamic simulation variables

T_{sw} : Torque at steering wheel(N-m)
δ_{swDD} : Angular Acceleration at steering wheel(rad/s^2)
δ_{swD} : Angular Velocity at steering wheel (rad/s)
δ_{sw} : Angular displacement of steering wheel(rad)
δ_{sc} : Angular displacement of steering column(rad)
δ_{T} : Angular displacement of torsion bar(rad)
δ_{P} : Angular displacement of pinion (rad)
δ_{VALVE} : Rotational displacement of input

* UC, Davis 대학원
** 정회원, 전북대학교 기계공학과

shaft to power steering unit (rad)

Y_RDD : Transitional Acceleration on the steering rack (m/s^2)

Y_RD : Transitional Velocity on the steering rack (m/s)

Y_R : Transitional displacement on the steering rack (m)

δ_{SLU1} : Rotational displacement of upper steering linkage on the passenger side kingpin (rad)

δ_{SLU2} : Rotational displacement of upper steering linkage on the driver side kingpin (rad)

δ_{SLL1} : Rotational displacement of lower steering linkage on the passenger side kingpin (rad)

δ_{SLL2} : Rotational displacement of lower steering linkage on the driver side kingpin (rad)

$\delta_{FW1}DD$: Angular Acceleration of the passenger side road wheel (rad/s^2)

$\delta_{FW1}D$: Angular Velocity of the passenger side wheel (rad/s)

δ_{FW1} : Angular displacement of the passenger side road wheel (rad)

$\delta_{FW2}DD$: Angular Acceleration of the driver side road wheel (rad/s^2)

$\delta_{FW2}D$: Angular Velocity of the driver side road wheel (rad/s)

δ_{FW2} : Angular displacement of the driver side road wheel (rad)

ϕ : Roll angle of vehicle (rad)

T_{K1} : Torque at passenger side kingpin (N-m)

T_{K2} : Torque at driver side kingpin (N-m)

AT_1 : Aligning torque of the passenger side road wheel (N-m)

AT_2 : Aligning torque of the driver side road wheel (N-m)

F_{PS} : Power steering assist force on the rack (N)

where,D : Differential operator (d/dt)

Measured or Estimated Steering System Parameters

B_{SW} : Upper Steering Column viscous damping coefficient (N-m/rad/s)

I_{SW} : Moment of Inertia of steering wheel ($N-m/rad/sec^2$)

K_{SC} : Steering column rotational stiffness (N-m/rad)

K_T : Rotational stiffness of power steering torsion spring on variable flow valve (N-m/rad)

N_G : Steering gear ratio of rotation of upper column to pinion shaft (unity in the rack and pinion system) (rad/rad)

R_P : Radius of pinion (m)

M_R : Steering rack mass

N_L : Front steering linkage rate on driver side from displacement to rack road wheel angle

K_{SL1} : Front passenger side steering rotational stiffness due to linkage and bushing

K_{SL2} : Front driver side steering rotational stiffness due to linkage and bushing

I_{FW1} : Inertia of right wheel and rotation mass about steering displacement

I_{FW2} : Inertia of left wheel and rotation mass about steering displacement

$B_{SL1,2}$: Viscous damping at each steering linkage bushing

B_R : Viscous damping of steering rack linear motion

CF_R : Coulomb friction breakout force on steering rack

CF_{FW} : Coulomb friction breakout force on road wheel

ε : Roll steer coefficient

η_F : Gear ratio efficiency of forward torque transmission

η_B : Gear ratio efficiency of backward torque transmission

η_{PS} : Efficiency of the power steering system due to hydraulic losses

A_{PIST} : Power steering pump effective piston area

1. Introduction

Ever since Segel[1] described the lateral vehicle responses combining the mathematical steering system model with the vehicle equations of motion,[2,3] his work has been used in other studies over the past three decades. Segel found that when the steering system model is incorporated into the vehicle equations of motion in handling studies, a more precise theoretical computation of the front wheel angular displacement is obtained. He also demonstrated how an unrestrained steering system and its dynamic behavior effects the static directional stability of the vehicle.

Recently, Mabrouka[4] incorporated a mathematical model of the steering mechanism into the vehicle's equations of motion to obtain a more suitable study of the vehicle directional control and stability and to investigate the influence of the steering system characteristics on the handling degrees of freedom transient responses. Rupp[5] represented a full model of an automotive steering system with both manual and power assisted configurations to better understand the interactions of the steering system dynamics with the vehicle dynamics.

2. Power Steering System Model Overview

Fig.1 shows the schematic diagram of the power steering system dynamic model. The full dynamic mathematical model of this power steering system configuration consists of a lumped mechanical system with 4 DOF ; the rotational displacement of the steering wheel, transitional displacement of the steering rack, and the rotational displacement of both road wheels about their each kingpin axis.

The equations of motion that will be developed for the steering system use the basic concept of compliance elements to transmit torque information to each successive element in the steering model. This model is composed of four lumped masses and inertia elements. These lumped terms are made up

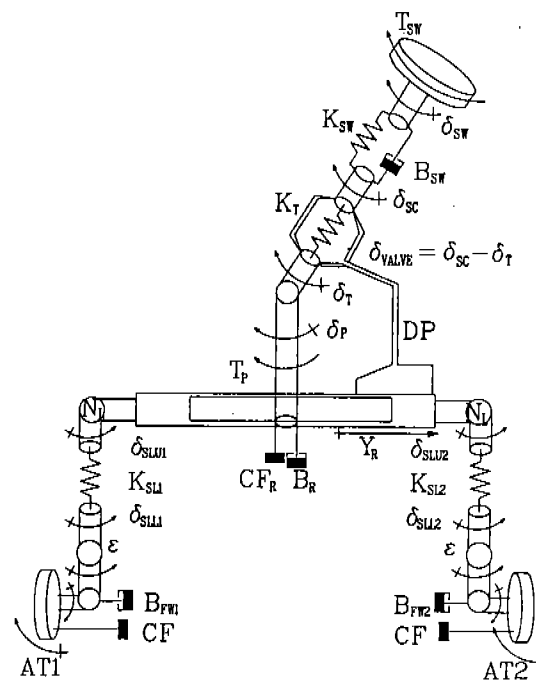

Fig.1 Schematic of the Dynamic Power Steering System Model

of the inertia at the steering wheel, inertia at the right and left wheel assemblies about their respective kingpin axis, and the effective mass of the steering rack having transitional motion. A combined total of nine rotational and one transitional dynamic dislacements are used in the developed steering model.

3. Mathematical Derivation of The Power Steering System Dynamics

Summation of the dynamic torques at the steering wheel yields

$$I_{sw}\ddot{\delta}_{SW} = T_{SW} - K_{SC}(\delta_{SW} - \delta_{SC}) - B_{SW}(\dot{\delta}_{SW} - \dot{\delta}_{SC}) \quad (1)$$

Summing the dynamic torques on each front wheel

$$I_{FW1}\ddot{\delta}_{FW1} = K_{SL1}(\delta_{SLU1} - \delta_{SLL1}) - AT_1 - B_{SL1}\dot{\delta}_{FW1} - CF_{FW}\times sgn(\dot{\delta}_{FW1}) \quad (2)$$

$$I_{FW2}\ddot{\delta}_{FW2} = K_{SL2}(\delta_{SLU2} - \delta_{SLL2}) - AT_2 - B_{SL2}\dot{\delta}_{FW2} - CF_{FW}\times sgn(\dot{\delta}_{FW2}) \quad (3)$$

where the sgn ($\dot{\delta}_{FW}$) terms in equations (2) and (3) accounts for the sign change of the front wheel angular velocity $\dot{\delta}_{FW}$; and AT_1 and AT_2 stand for the tire aligning torque produced by tire forces which are generated at the tire-road interface during steering and rolling action.

Each of the summed torque equations in the rack motions can be represented by applying Newton's second law and dividing by the linkage rate, N_L, or pinion radius values. The front steering linkage rate on the driver side is the same as the one on the passenger side, since the steering linkage is assumed to be symmetric in the model. The summation of all the forces is the following,

$$M_R\ddot{Y}_R = \eta_F\frac{T_P}{R_P} - \eta_B\frac{T_{K1}}{N_L} - \eta_B\frac{T_{k2}}{N_L} - B_R\dot{Y}_R - \eta_{PS}F_{PS} - CF_R \times sgn(\dot{Y}_R) \quad (4)$$

where η_F represents the torque-transmission efficiency of the gearbox which can be set equal to unity in the rack-and-pinion steering gear, η_B the backward torque-transmission efficiency and η_{PS} the efficiency of the power steering system due to hydraulic losses. F_{PS} accounts for a power steering assist force on rack, and $\ddot{Y}_R$ the transitional acceleration of the rack mass. Equations (1), (2), (3), and (4) represent the 4 DOF for the steering system model. A steady state analysis useful for the computer simulation was discussed in this research. The mathematical derivation was described by Jang[6] in detail. Thus, equations (1), (2), (3), and (4) become as follows, respectively.

$$\begin{aligned} I_{SW}\ddot{\delta}_{SW} = {} & T_{SW} - B_{SW}(\dot{\delta}_{SW} - \dot{\delta}_{SC}) \\ & + \left\{\frac{\left(\frac{\eta_B R_P K_{SL1}}{N_L}\right)}{DEN}\right\}\delta_{FW1} + \left\{\frac{\left(\frac{\eta_B R_P K_{SL2}}{N_L}\right)}{DEN}\right\}\delta_{FW2} \\ & + \left\{\frac{K_{SC}\left[\frac{\eta_B R_P^2(K_{SL1}-K_{SL2})}{N_L^2 K_T}+1\right]}{DEN} - K_{SC}\right\}\delta_{SW} \\ & - \left\{\frac{\left[\frac{\eta_B R_P(K_{SL1}+K_{SL2})}{N_L}\right]}{DEN}\right\}\varepsilon\phi - \left\{\frac{\eta_{PS}R_P}{DEN}\right\}F_{PS} \end{aligned} \quad (5)$$

where,

$$DEN = \left[\frac{\eta_B R_P^2(K_{SL1}+K_{SL2})}{N_L^2 K_{SC}} + \frac{\eta_B R_P^2(K_{SL1}+K_{SL2})}{N_L^2 K_T} + 1\right]$$

$$I_{FW1}\ddot{\delta}_{FW1}=-AT_1-B_{SL1}\dot{\delta}_{FW1}-CF_{FW}\times sgn(\dot{\delta}_{FW1})$$
$$+\left\{\frac{\frac{R_PK_{SL1}}{N_L}(1+\frac{K_{SC}}{K_T})\left(\frac{\eta_BR_PK_{SL1}}{N_LK_{SC}}\right)}{[DEN]}-K_{SL1}\right\}\delta_{FW1}$$
$$+\left\{\frac{\frac{R_PK_{SL1}}{N_L}(1+\frac{K_{SC}}{K_T})\left(\frac{\eta_BR_PK_{SL2}}{N_LK_{SC}}\right)}{[DEN]}-K_{SL1}\right\}\delta_{FW2}$$
$$+\left\{\frac{\frac{R_PK_{SL1}}{N_L}(1+\frac{K_{SC}}{K_T})\left[\frac{\eta_BR_P^2(K_{SL1}+KSL2)}{N_L^2K_T}+1\right]}{[DEN]}\right.$$
$$\left.-\frac{R_PK_{SC}K_{SL1}}{N_LK_T}\right\}\delta_{SW}$$
$$+\left\{\frac{\frac{R_PK_{SL1}}{N_L}(1+\frac{K_{SC}}{K_T})\left(-\frac{\eta_BR_P(K_{SL1}+KSL2)}{N_L^2K_T}\right)}{[DEN]}+K_{SL1}\right\}\varepsilon\phi$$
$$+\left\{\frac{\frac{R_PK_{SL1}}{N_L}(1+\frac{K_{SC}}{K_T})\left(-\frac{\eta_{PS}R_P}{K_{SC}}\right)}{[DEN]}\right\}F_{PS} \quad (6)$$

$$I_{FW2}\ddot{\delta}_{FW2}=-AT_2-B_{SL2}\dot{\delta}_{FW2}-CF_{FW}\times sgn(\dot{\delta}_{FW2})$$
$$+\left\{\frac{\frac{R_PK_{SL2}}{N_L}(1+\frac{K_{SC}}{K_T})\left(\frac{\eta_BR_PK_{SL1}}{N_LK_{SC}}\right)}{[DEN]}\right\}\delta_{FW1}$$
$$+\left\{\frac{\frac{R_PK_{SL2}}{N_L}(1+\frac{K_{SC}}{K_T})\left(\frac{\eta_BR_PK_{SL2}}{N_LK_{SC}}\right)}{[DEN]}-K_{SL2}\right\}\delta_{FW2}$$
$$+\left\{\frac{\frac{R_PK_{SL2}}{N_L}(1+\frac{K_{SC}}{K_T})\left[\frac{\eta_BR_P^2(K_{SL1}+KSL2)}{N_L^2K_T}+1\right]}{[DEN]}\right.$$
$$\left.-\frac{R_PK_{SC}K_{SL2}}{N_LK_T}\right\}\delta_{SW}$$
$$+\left\{\frac{\frac{R_PK_{SL2}}{N_L}(1+\frac{K_{SC}}{K_T})\left(-\frac{\eta_BR_P(K_{SL1}+KSL2)}{N_L^2K_T}\right)}{[DEN]}+K_{SL1}\right\}\varepsilon\phi$$
$$+\left\{\frac{\frac{R_PK_{SL2}}{N_L}(1+\frac{K_{SC}}{K_T})\left(-\frac{\eta_{PS}R_P}{K_{SC}}\right)}{[DEN]}\right\}F_{PS} \quad (7)$$

We now turn our attention to equations (5) through (8). These four equations represent the 4 DOF of the steering system, where $\ddot{Y}_R$ can be expressed as a function of the steering wheel angular displacement δ_{sw}, and each road wheel angular displacement, δ_{fw1}, and. δ_{fw2}. The above four equations are very useful for handling studies where the steering system dynamics are connected to the vehicle body dynamics. Segel[1] derived a 3 DOF automotive model for lateral dynamic properties of the vehicle to steering control. In this paper, a linear vehicle handling model with a first order lagged lateral forces developed by Heydinger[2] is used.

4. Power Assist Force Measurement

The power steering boost curve was determined by measuring the torque at the torsion bar and tierod forces on both linkages as the torsional bar valve is twisted during a vehicle test. By slowly increasing the steering wheel angle, while recording the steering wheel torque and tierod forces, the pressure boost curve can be obtained from the following relationship:

$$M_R\dot{Y}_R=-B\dot{Y}_R-CF_R\times sgn(\dot{Y}_R)$$
$$-\left\{\left[\frac{\eta_BR_P(K_{SL1}+K_{SL2})}{N_L^2}+\frac{\eta_BR_PK_{SC}(K_{SL1}+K_{SL2})}{N_L^2K_T}+\frac{K_{SC}}{R_P}\right]\left[\frac{\left(\frac{\eta_BR_PK_{SL1}}{K_{SC}}\right)}{[DEN]}\right]-\frac{\eta_BK_{SL1}}{N_L}\right\}\delta_{FW1}$$
$$-\left\{\left[\frac{\eta_BR_P(K_{SL1}+K_{SL2})}{N_L^2}+\frac{\eta_BR_PK_{SC}(K_{SL1}+K_{SL2})}{N_L^2K_T}+\frac{K_{SC}}{R_P}\right]\left[\frac{\left(\frac{\eta_BR_PK_{SL2}}{K_{SC}}\right)}{[DEN]}\right]-\frac{\eta_BK_{SL2}}{N_L}\right\}\delta_{FW2}$$
$$-\left\{\left[\frac{\eta_BR_P(K_{SL1}+K_{SL2})}{N_L^2}+\frac{\eta_BR_PK_{SC}(K_{SL1}+K_{SL2})}{N_L^2K_T}+\frac{K_{SC}}{R_P}\right]\left[\frac{\left[\frac{\eta_BR_P^2(K_{SL1}+K_{SL2})}{N_L^2K_T}\right]}{[DEN]}\right]-\frac{K_{SC}}{R_P}-\frac{\eta_BR_PK_{SC}(K_{SL1}+K_{SL2})}{N_L^2K_T}\right\}\delta_{SW}$$
$$+\left\{\left[\frac{\eta_BR_P(K_{SL1}+K_{SL2})}{N_L^2}+\frac{\eta_BR_PK_{SC}(K_{SL1}+K_{SL2})}{N_L^2K_T}+\frac{K_{SC}}{R_P}\right]\left[\frac{\left[\frac{\eta_BR_P(K_{SL1}+K_{SL2})}{N_LK_{SC}}\right]}{[DEN]}\right]-\frac{\eta_P(K_{SL1}+K_{SL2})}{N_L}\right\}\varepsilon\phi$$
$$+\left\{\left[\frac{\eta_BR_P(K_{SL1}+K_{SL2})}{N_L^2}+\frac{\eta_BR_PK_{SC}(K_{SL1}+K_{SL2})}{N_L^2K_T}+\frac{K_{SC}}{R_P}\right]\left[\frac{\frac{\eta_{PS}R_P}{K_{SC}}}{[DEN]}\right]-\eta_{PS}\right\}F_{PS} \quad (8)$$

$$\frac{T_P}{R_P} = \text{Tierod\_Forces} + F_{ps}(\text{PowerAssist Force}) \quad (9)$$

where R_P is the pinion gear pitch radius, and T_P is the measured torque in the steering column.

Fig.2 shows the pressure boost curve at two different speeds as the steering wheel is turned against the rack. The displacement of the torsional bar angle needs to be zeroed from the initial point of contact against the rack. With this information, the curve can be replotted with the zeroed pressure versus the zeroed valve displacement. A eighth order polynomial curve fit was used to provide sufficient match of the experimental data. Fig.2 shows a curve-fit of the experimental data to form the pressure boost curve for torsion bar valve displacement. The implementation of the power assist force, F_{PS}, on the rack is shown in the next equation:

$$F_{PS} = \{C_1\delta_V^8 + C_2\delta_V^7 + C_3\delta_V^6 + C_4\delta_V^5 + C_5\delta_V^4 + C_6\delta_V^3 + C_7\delta_V^2 + C_8\delta_V + C_9\} * A_{\text{piston area}} \quad (10)$$

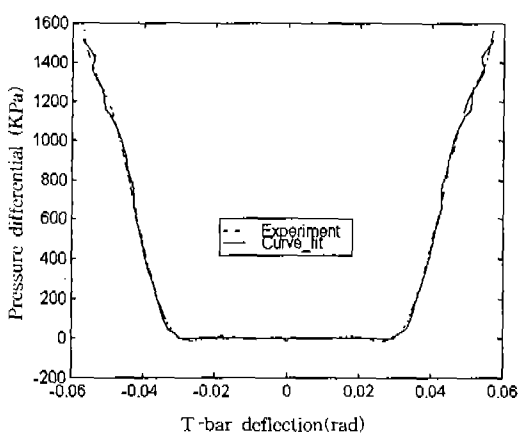

Fig.2 Pressure Boost Curve

where,

C_1 = 4.7097E+11, C_2 = 5.6380E+10,
C_3 = -1.1864E+10, C_4 = -1.1362E-05,
C_5 = 8.093E+07, C_6 = 6.8698E-08,
C_7 = 3.47191E+05, C_8 = -9.8992E-11
C_9 = -115.9779

5. Results and Discussions

The results for the steady-state time domain comparison are generated using J-turn maneuvers. The simulated resulted were obtained using the same angular displacement step input as was experimentally measured during the field test to generate the desired lateral acceleration level.

All the experimental results were obtained from the 1994 Ford Taurus GL. At low speed, the lateral acceleration become close to the experimental result and this also happens in the responses to slowly increasing steer inputs. At higher speeds, the lateral acceleration values are a little higher than the experimental values. Fig.3 shows a good agreement at two different vehicle speeds. Notice that the lateral acceleration is a function of yaw rate and forward speed. Thus, we are going to look at the yaw rate responses.

This yaw rate prediction of the vehicle is an important characteristic for validation of the developed steering model, because it is largely dependent on the developed steering model. Simulation yaw rate response to a steering input can only accurately predict actual vehicle behavior if many vehicle attributes are correctly modeled. The field tests provide a good match with the yaw rate predictions from the simulation runs as shown in Fig.4.

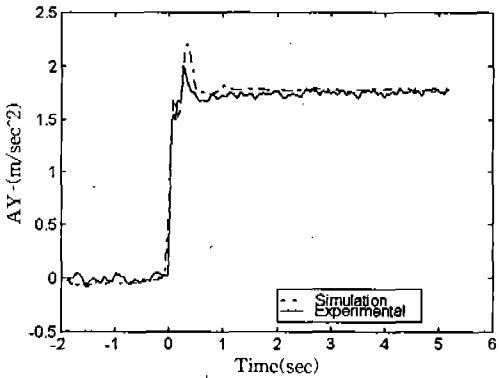

(a) from +0.2g J-Turn Maneuver at 11.2m/s

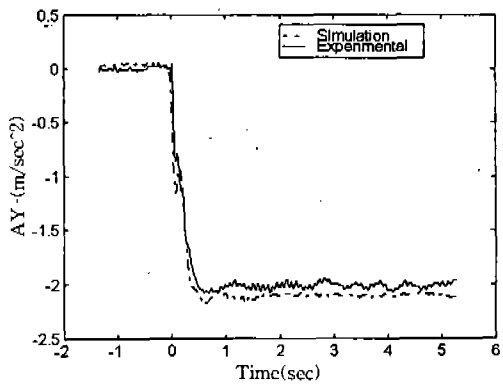

(b) from -0.2g J-Turn Maneuver at 22.7m/s

Fig.3 Lateral Acceleration Responses

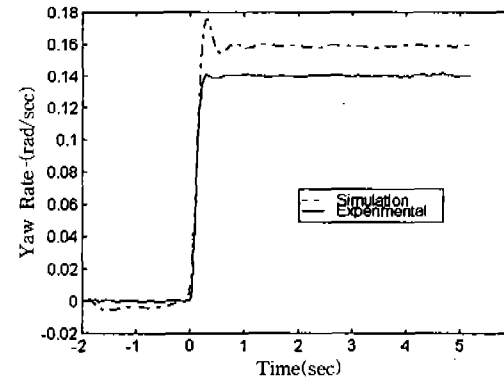

(a) from +0.2g J-Turn Maneuver at 11.2m/s

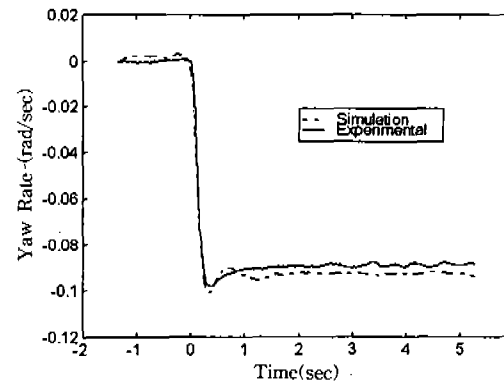

(b) from -0.2g J-Turn Maneuver at 22.7m/s

Fig.4 Yaw Rate Responses

Fig.5 shows the comparison between the simulation predictions and experimental data for the on-center transition test. These are on-center transition test and on-center weave test.

Fig.6 can explain the characteristics of the torsion bar twist and power assist force. As shown in Fig.5 and Fig.6, the torsion bar deflection follows the shape of the steering input. The power assist force shows that the steering system provides the positive force in all cases since when the value angle opens being affected by the torsion bar deflection. The power assist force provide 0 N when there is a switch between the torsion bar deflections as shown in Fig.5 and Fig.6.

6. Conclusions

This research has provided for a better understanding of vehicle handling dynamics and the mathematical equations considering the steering system nonlinearities. The developed mathematical model for the steering system dynamics has shown good simulation predictions and advanced the state-of-the-art of vehicle dynamics simulation.

A methodology developed by Heydinger[2] to evaluate the simulations was used in the computer simulation evaluation by using the repeated experimental runs at each test condition to improve the confidence of the experimental data.

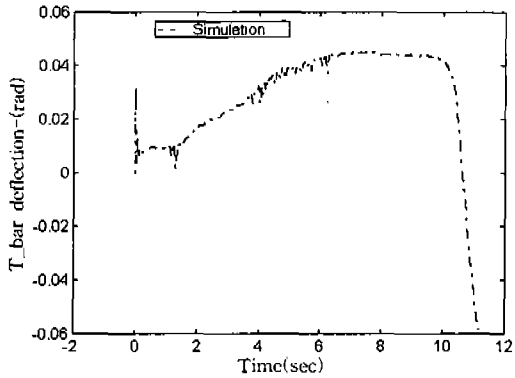

(a) Simulation of Torsion Bar Deflection (rad)

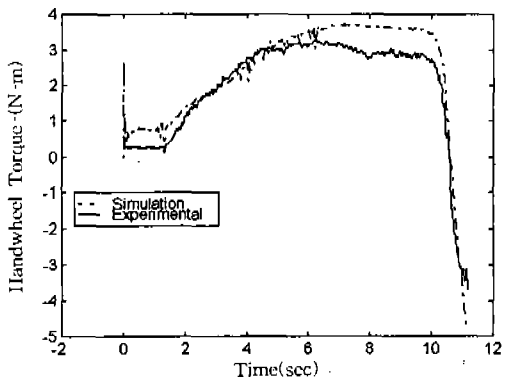

(b) Steering wheel Torque (N-m)

Fig.5 Vehicle Dynamic Responses from On-Center Transition Test at 22m/s

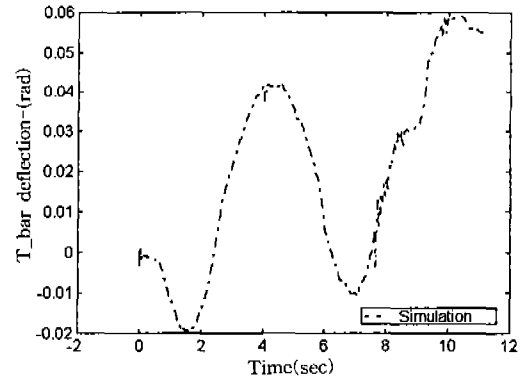

(a) Simulation of Torsion Bar Deflection (rad)

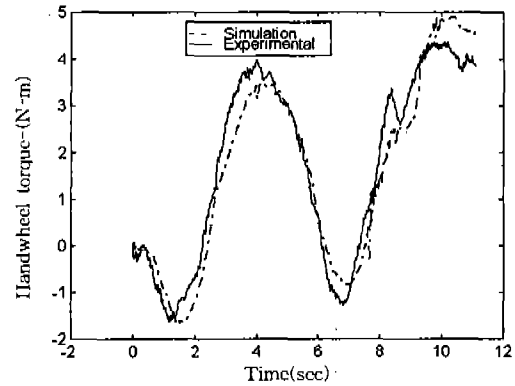

(b) Steering wheel Torque (N-m)

Fig.6 Vehicle Responses to On-Center Weave Test at 22m/s

For all simulations, the experimentally mea-sured steering wheel angle and averaged vehicle speed were used as inputs. This simulation with the experimental measured inputs provides the best validation of the model during the full scale vehicle testing.

References

1. Segel, L., "Theoretical Prediction and Experimental Substantiation of the Response of the Automobile to Steering Control", Research in Automobile Stability and Control in Tire Performance, Proceedings of the Automobile Division, The Institution of Mechanical Engineers, No.7, pp. 26~46, 1967.
2. Heydinger, G. J., "Improved Simulation and Validation of Road Vehicle Handling Dynamics", Ph.D. Dissertation, The Ohio State University, 1990.
3. Doebelin, E. O., "System Modeling and Response-Theoretical and Experimental Approaches", Chpt.12, The Ohio State University, pp. 475~526, 1980.
4. Mabrouka, H., "Effect of Lateral Tire Flexibility on the Steering System Dynamic Behavior", M.S. Thesis, The Ohio State University, 1994.
5. Rupp, M. Y., "Passive Dynamics Steering

System Model For Use in Vehicle Dynamics Simulation", M.S. Thesis, The Ohio State University, 1994.
6. Jang, B. C., "A Mathematical Model of A Power Steering System For Implementation In A Driving Simulator," M.S. Thesis, The Ohio State University, 1996.
7. Chrstos, J.P., "Use of Vehicle Dynamics Modeling to Quantify Race Car Handling Behavior", Ph.D. Dissertation Proposal, The Ohio State University, 1995.